agriculture

MDPI

Article

Design of a Spring-Finger Potato Picker and an Experimental Study of Its Picking Performance

Lihe Wang [1,2], Fei Liu [1,*], Qiang Wang [3], Jiaqi Zhou [1], Xiaoyu Fan [1], Junru Li [1], Xuan Zhao [1] and Shengshi Xie [1]

[1] College of Mechanical and Electrical Engineering, Inner Mongolia Agricultural University, Hohhot 010010, China; 18326106301@163.com (X.F.)
[2] Vocational and Technical College, Inner Mongolia Agricultural University, Baotou 014109, China
[3] Agricultural and Animal Husbandry Technology Extension Centre, Hohhot 010010, China
* Correspondence: afei2208@imau.edu.cn

Abstract: To address the problems of low pickup rates and high rates of wounds in the mechanised harvesting of potatoes under sectional harvesting conditions, a spring-finger potato picker was designed and its overall structure and working principles were described. The kinematic principle of the spring-finger was analysed based on the picking constraints, and the kinematic parameters of the picker were determined. A response surface Box–Behnken Design test design was used to carry out a quadratic orthogonal rotational test, with the speed of the spring-finger, the forward speed of the machine, and the embedded depth as test factors, and the loss rate and the wounded potato rate as evaluation indicators. The test results were optimised and analysed. When the spring-finger speed was 19.57 r/min, the forward speed was 0.61 m/s and the embedded depth was 71.31 mm, the loss rate was 1.18%, and the wounded potato rate was 5.71%. The optimised data were verified, and the results showed that the loss rate of the spring-finger potato picker was 1.48% and the wounded potato rate was 4.98%, meeting the potato picking and harvesting requirements. The research can provide a theoretical basis and design reference for the development and application of sectional potato harvesting machinery.

Keywords: agricultural machinery; harvesting; potato; spring-finger; ADAMS-EDEM; loss rate; wounded potato rate

Citation: Wang, L.; Liu, F.; Wang, Q.; Zhou, J.; Fan, X.; Li, J.; Zhao, X.; Xie, S. Design of a Spring-Finger Potato Picker and an Experimental Study of Its Picking Performance. *Agriculture* **2023**, *13*, 945. https://doi.org/10.3390/agriculture13050945

Academic Editors: Cheng Shen, Zhong Tang and Maohua Xiao

Received: 17 March 2023
Revised: 18 April 2023
Accepted: 22 April 2023
Published: 25 April 2023

1. Introduction

The potato is one of the most widely grown crops worldwide due to its high yield and unique nutritional value [1]. In 2015, China categorized the potato as a strategic staple food; under the development process of the national grain growing industry structure adjustment and potato staple food strategy, China's potato planting area and total production have become some of the best in the world. Potatoes are planted all over the country, with both planting area and total production on the increase. Although China's potato planting mechanization level is improving year by year, the potato harvest mechanization level is still very low; the potato machine harvesting rate is less than 50%, which has seriously restricted the development of China's potato industry [2–4]. At present, potato machine harvesting methods can be divided into combined and sectional harvesting according to the differences in the harvesting process. In China, potatoes are generally eaten fresh, for reasons such as dietary structure [5]. Potatoes harvested with combine harvesters have fragile skins, high trash content and are not easily stored for long periods, so potato harvesting in China is still mainly done in sections [6]. It is important to develop efficient and low-loss potato harvesting equipment to meet the customary consumption and harvesting methods of potatoes in China.

In order to solve the problems of manual potato picking with high labour intensity and low production efficiency, researchers have done a lot of research and achieved good

application results. Shi et al. [7] designed a small potato picker with a 30 kw tractor, using a picking shovel combined with a spring-fingered bar conveyor chain to achieve potato picking, and a potato block lifting device and a potato block collection device to achieve potato soil separation and potato block collection, but the wounded potato rate and the rate of contamination are higher than the relevant national industry standards. Xiao et al. [8] designed a small potato picking and grading harvester, using a roller-type potato secondary grading device to achieve combined potato picking, grading and potato block collection, but the number of grading levels does not meet the actual grading requirements, and the picking efficiency is low. Hu et al. [9] designed an integrated potato picking and grading harvester, using a cam mechanism and a vibration dampening lever of the wheel mechanism to achieve horizontal and vertical vibration of the screening part, thus achieving the purpose of potato two-monopoly picking and three-stage sorting, but the size of the whole machine increased, causing a little problem for the machine's turning and turning around. Liu et al. [10] designed a potato harvester with drum-type separation, using a rotary-driven digging device arranged in a circle, while using a drum sieve-type separation structure to separate the conveying device, but there were certain problems of broken skins and injured potatoes. Wang [11] designed an active turntable potato picking device and developed a picking mechanism test stand to carry out exploratory trials in a digitised soil trough, but there was still a certain amount of potato leakage and soil congestion. Yang et al. [12] designed the 4UJ-1400 potato picker, which used a forced pushing device to lift potatoes at a large angle, with good soil removal effects, but low picking efficiency. Wei et al. [13] designed a crawler self-propelled sorting potato harvester, using crawler self-propelled technology, automatic row digging technology and a combination of screen surface separation and manual assisted sorting to achieve potato harvesting, but there are certain problems of potato leakage and wounded, which has not yet been transformed into a popular product.

This paper addresses the problems of low picking rates and high wounded potato rate in mechanised potato harvesting under sectional harvesting conditions, and designs a spring-finger potato picker, analyses the theoretical calculations of its key components, establishes the kinetic equations of the spring-finger in the picking process, and determines the optimal operating parameters through laboratory test in the hope of reducing the loss and wounded potato rates during sectional potato picking.

2. Materials and Methods

2.1. Overall Structure and Working Principles

2.1.1. Overall Structure

The spring-finger potato picking device is mainly composed of a spindle, a spring-finger shaft, a crank, a curved cover, a roller, a spring-finger, and a roller disc, as shown in Figure 1. The device has three sets of spring-finger, with each set evenly distributed on the spring-finger shaft. The crank is connected at one end to the roller and at the other end to the spring gear shaft that passes through the drum disc. As the roller rolls in the cam chute, the crank pushes the spring gear shaft to move the spring-finger along a set course. The curved hood is directly connected to the frame at one end and the other end is staggered with the spring-finger to prevent debris from entering the pickup.

2.1.2. Principle of Operation

The motion of the spring-finger in the picking mechanism is a combination of linear motion in the direction of operation of the machine and rotary motion controlled by a cam slide. The cam chute constrains the movement of the rollers and at the same time constrains the different attitudes of the spring-finger during rotation, the different picking attitudes of the spring-finger correspond to different picking phases. For each week of rotation of the roller in the cam slide, the picking spring-finger correspond to four phases, i.e., "pickup", "lifting", "push" and "quick-return". The pickup cycle is shown in Figure 2.

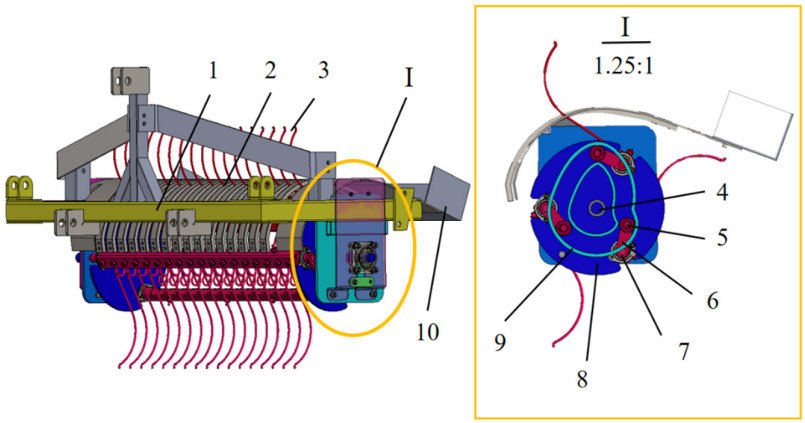

Figure 1. Schematic diagram of the complete assembly of the picking device: (1) frame (2) curved housing (3) popping gear (4) spindle (5) roller (6) crank handle (7) spring-finger shaft (8) roller disc (9) inner and outer cam (10) potato collection box.

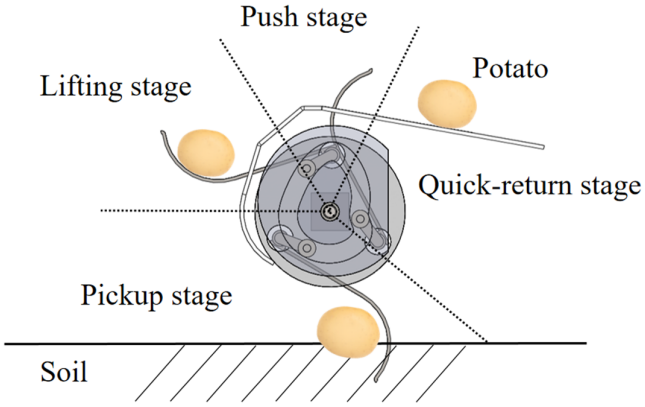

Figure 2. Diagram of the spring-finger picking process.

(1) Pickup stage: at the start of the pickup phase, the drum rotates and at the same time moves the spring-finger underneath the drum, the end of the spring-finger start to protrude through the gap in the curved hood and then are inserted into the ground at a certain angle of entry, then the spring-finger continue to move, as the machine advances and the drum disc rotates, the spring-finger continue to move upwards to pick up the potatoes laid on the ground.

(2) Lifting stage: at the start of the lifting stage, the direction of spring-finger swing is controlled by the rollers in the cam chute and the lifting stage starts in a horizontal position. The drum disc continues to rotate and the end of the spring-finger begin to move backwards and upwards, transporting the pickup potatoes to the top of the curved hood.

(3) Push stage: the phase starts with the pickup spring-finger located at the back front, the relative speed direction is horizontal backwards, pushing the potatoes backwards, in the pushing phase, the pickup spring-finger and the drum disc maintain a large backward angle of inclination between the pickup spring-finger and the curved hood shell to prevent a clamping angle between the pickup spring-finger and the curved hood shell, which is not conducive to backward movement of the potatoes or wounded potato to the potatoes.

(4) Quick-return stage: after the pickup spring-finger have finished picking up, lifting, pushing and unloading potatoes, with the continuous rotation of the drum disc, there is an idling stage before the spring-finger return to the initial position of the pickup stage, this stage does not touch the potatoes and the ground, but the spring-finger rotate with great acceleration in order to quickly return to the starting position of the next pickup stage, shortening the rush back stage and improving the pickup rate.

2.2. Design of Key Components

2.2.1. Spring-Finger

During sectional harvesting, potatoes are excavated and laid out to dry in the field; the distribution is haphazard and irregular, as shown in Figure 3. Potatoes that are excavated and mixed with clods of mud, roots and stems, etc., are exposed on the ground as bright potatoes; meanwhile, others are completely or partially buried in the ground and are known as dark potato [14]. Potatoes are excavated and distributed either on the surface or at a depth of 30–50 mm from the surface [15]. The depth of the pickup tines should be designed to pick up as many potatoes as possible, ensuring that dark potatoes can also be picked up without difficulty, and avoiding soil congestion and severe wear on the tines as a result of going too deep into the soil. Based on the above distribution of potatoes after excavation, the embedded depth should be limited to between 60 and 80 mm to meet the potato pickup requirement. In addition, the mechanical characteristics of the spring-finger should also be taken into account during the design process, as the ground is uneven and mixed with debris in the field due to the constraints of the picking operation.

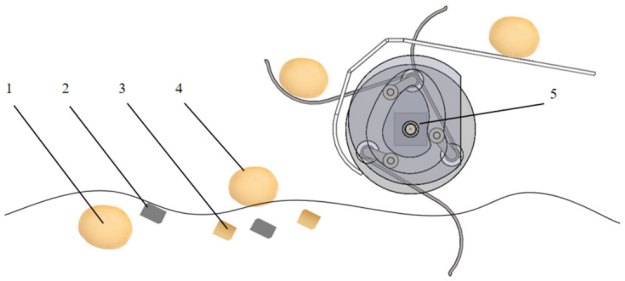

Figure 3. Potato distribution status: (1) dark potato (2) soil block (3) stone block (4) potato (5) pickup device.

The design of the angle of entry of the pickup tines is a function of the pickup effect and is based on the need to pick up potatoes smoothly while reducing wounded potato to the potatoes and not digging up too much soil, in order to reduce the forces on the pickup tines [16]. The potato is analysed for forces, as shown in Figure 4, and the relationship (1) is detailed.

$$\begin{cases} F_N sin\alpha + F_J cos\alpha - F - f cos\alpha = 0 \\ F_N cos\alpha - F_J sin\alpha - \mathrm{mg} + f sin\alpha = 0 \end{cases} \quad (1)$$

where F is the resistance of the potato in the soil, N; m is the mass of the potato, kg; F_N is the support force of the potato with the spring-finger, N; f is the friction force, N; and α is the angle between F and f, °; F_J is the centripetal force on the potato, N; g is the acceleration of gravity, N/kg.

The relevant parameters are brought into the above equation to calculate the pickup spring-finger entry angle $\alpha \geq 53°$. This range ensures that potatoes enter the picker spring-finger smoothly, minimising the wounded potato rate and avoiding the high picking resistance caused by a large angle of entry, thus increasing efficiency and reducing consumption. After determining the lug depth and lug angle, the maximum length that the spring-finger can extend out of the picker is initially determined to be 200 mm, the total length of the spring-finger is 260 mm, the bending angle of the spring-finger δ is 120°, and the material chosen is 65 Mn. The structure of the spring-finger is shown in Figure 5.

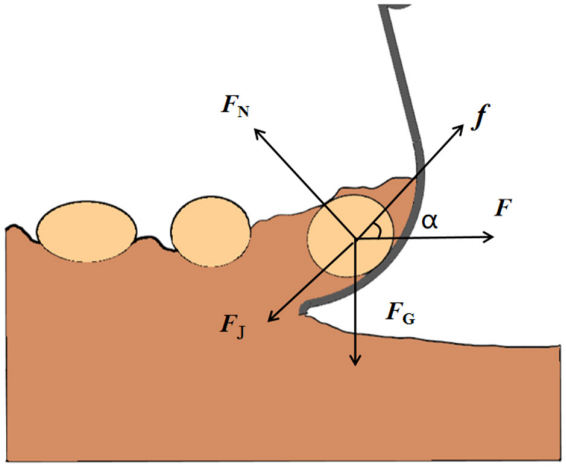

Figure 4. Potato force analysis diagram.

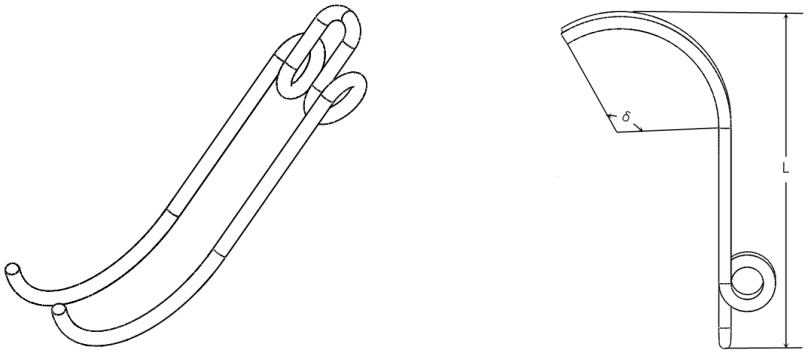

Figure 5. Schematic diagram of the spring-finger structure: (**a**) axonometric drawings. (**b**) side view.

The design of the pickup spacing of the spring-finger should be based on the physical characteristics of the potatoes and their pickup characteristics. The potatoes grown in China are excavated and harvested and then laid on the surface. According to their distribution on the surface, the potatoes are excavated and laid out in an orderly manner, and the grouping state is irregular.

2.2.2. Roller Discs

The picking device is driven by the main drive shaft to rotate the drum disc to rotate the spring-finger shaft, thus completing the picking work. The size of the radius of the drum disc does not directly affect the spring-finger movement, but the size of the drum disc determines the size of the whole machine. Referring to agricultural machinery manuals and other similar picking devices in China, the final diameter of the drum is determined to be 320 mm. The structure of the drum is shown in Figure 6.

2.2.3. Cranks and Rollers

Depending on the movement characteristics of the crank linkage, the crank length should not be designed to be too long or too short. A crank that is too long may result in the rollers becoming stuck in the cam slide and not moving continuously. Meanwhile, a crank that is too short will result in the mechanism running less smoothly and with more impact on the cam slide. The crank is hinged to the roller at one end and pinned to the poppet shaft at the other end. With reference to various models of pickup devices, a crank length of 110 mm was finally chosen.

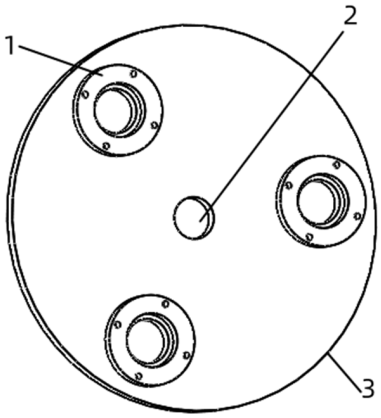

Figure 6. Schematic diagram of the structure of the roller disc: (1) spring gear shaft seat (2) central hole of the drive shaft (3) disc.

The size of the roller radius r_r should take into account the size of the cam slide. As the roller is rolling frictionally and is subjected to large forces when working, a small radius will lead to serious wear on the slide, and the roller is prone to deformation when the radius is too large. Therefore, the size of the rollers should therefore be designed to satisfy Equation (2):

$$r_r = (0.1 - 0.5)\, R_a \tag{2}$$

where R_a is the radius of the base circle, mm; r_r is the radius of the rollers, mm.

The final radius of the rollers was determined to be 45 mm, and the crank poppet shaft-fixing structure is shown in Figure 7.

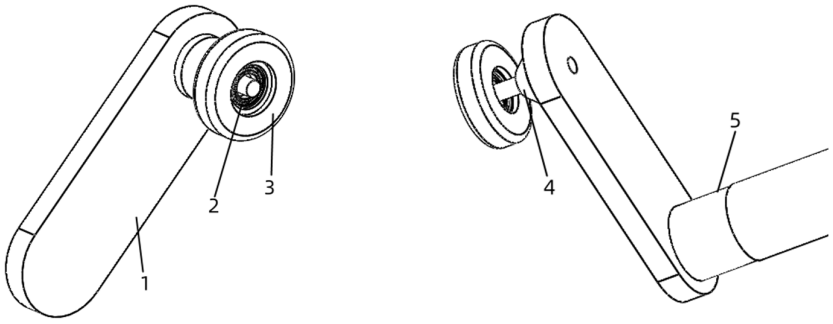

Figure 7. Fixed structure of the crank gear shaft: (1) crank (2) bearing (3) roller (4) connecting rod (5) gear shaft.

2.2.4. Cam Slides

According to the working principle of the picking device, the shape of the cam chute constrains the rotation pattern and attitude of the picking spring-finger during the picking process and is a decisive factor in picking quality. According to the theory of the "reversed pendulum follower disc cam mechanism" by Sheng Kai et al., the design of the cam chute centreline should correspond to the initial position and attitude of the picking spring-finger and the law of motion during the four picking stages [17,18]. The design is based on the polynomial law of motion of the cam slide curve, and a sketch of the picking mechanism based on this design method is shown in Figure 8.

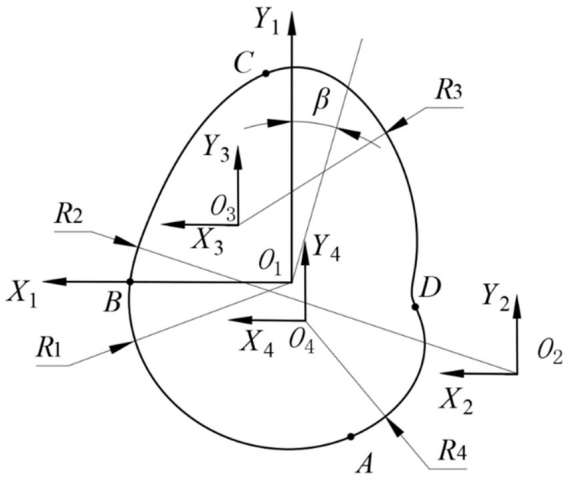

Figure 8. Sketch of the centreline analysis of the cam slide of the poppet pickup mechanism.

Based on the mechanism parameters, a sketch of the pop-up roller pickup mechanism was created in Auto CAD using a graphical method to obtain the phase angles $\beta_1 = 78.36°$, $\beta_2 = 89.15°$, $\beta_3 = 115.93°$, and $\beta_4 = 68.10°$ for the four stations.

As a result of the above analysis, it can be concluded that the cam slide centreline is composed of multiple circular sliding curves. The mathematical model of the cam slide centreline for each stage is established as follows.

(1) Pickup stage cam chute centreline model.

Curve segment $\overset{\frown}{AB}$ trajectory Equation (3):

$$\begin{cases} X = R_1 cos\beta \\ Y = R_1 sin\beta \end{cases} \tag{3}$$

where R_1 is the $\overset{\frown}{AB}$ radius, mm; β is the angle of the circle corresponding to the centreline of the cam slide, rad.

(2) Model of the centreline of the cam slipway during the lift stage.

Curve segment $\overset{\frown}{BC}$ trajectory Equation (4):

$$\begin{cases} X = R_2 cos\beta_{BC} - X_{O_2} \\ Y = R_2 sin\beta_{BC} - Y_{O_2} \end{cases} \tag{4}$$

where R_2 is the $\overset{\frown}{BC}$ radius, mm; β_{BC} is the angle of circularity of $\overset{\frown}{BC}$, rad; X_{O_2} is the value of the X-axis coordinates of point O_2, mm; Y_{O_2} is the value of the Y-axis coordinates of point O_2, mm.

(3) Model of the centreline of the cam slipway during the pushing stage.

Curve segment $\overset{\frown}{CD}$ trajectory Equation (5):

$$\begin{cases} X = R_3 cos\beta_{CD} + X_{O_3} \\ Y = R_3 sin\beta_{CD} + Y_{O_3} \end{cases} \tag{5}$$

where R_3 is the $\overset{\frown}{CD}$ radius, mm; β_{CD} is the angle of circularity of $\overset{\frown}{CD}$, rad; X_{O_3} is the value of the X-axis coordinates of point O_3, mm; Y_{O_3} is the value of the Y-axis coordinates of point O_3, mm.

(4) Model of the centreline of the cam slipway during the quick-return stage:

Curve segment $\overset{\frown}{DA}$ trajectory Equation (6):

$$\begin{cases} X = R_4 cos\beta_{DA} - X_{O_4} \\ Y = R_4 sin\beta_{DA} + Y_{O_4} \end{cases} \quad (6)$$

where R_4 is the $\overset{\frown}{DA}$ radius, mm; β_{DA} is the angle of circularity of $\overset{\frown}{DA}$, rad; X_{O_4} is the value of the X-axis coordinates of point O_4, mm; Y_{O_4} is the value of the Y-axis coordinates of point O_4, mm.

The final schematic diagram of the cam slide structure is shown in Figure 9.

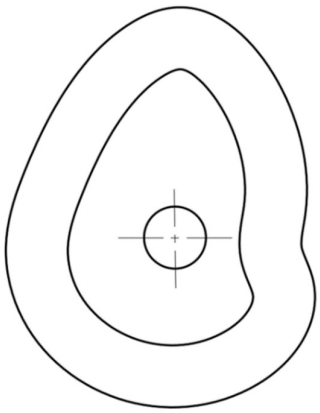

Figure 9. Schematic diagram of the cam slipway structure.

2.3. Analysis of the Principle of Spring-Finger Movement

The law of motion of the spring-finger roller picker is that the cam disk is not moving, the crank and the spring-finger connection point is fixed on the roller, the roller is rotating around the centre of rotation to drive the spring-finger movement. As shown in Figure 10, a coordinate system is established with the centre of the base circle of the cam mechanism as the origin O. The forward direction of the picker is the X-axis direction, and the direction perpendicular to the ground is the Y-axis direction, and the movement of the spring-finger is analysed.

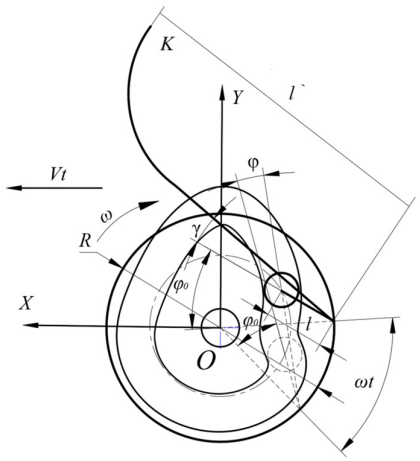

Figure 10. Cam of the spring-finger pickup mechanism: A is the crank and spring-finger connection point; B is the roller centrepoint; K is the spring-finger end point.

The displacement of the K point at the end of the spring-finger is shown in Equation (7):

$$\begin{cases} X = V_t t + Rcos\omega t - Lcos(\omega t + \varphi_0 + \varphi) + L'cos(\omega t + \varphi_0 + \varphi - \gamma) \\ Y = Rsin\omega t - Lsin(\omega t + \varphi_0 + \varphi) + L'sin(\omega t + \varphi_0 + \varphi - \gamma) \end{cases} \quad (7)$$

where X is the horizontal displacement of the end of the spring-finger, m; Y is the vertical displacement of the end of the spring-finger, m; V_t is the forward velocity, m/s; L is the length of the crank, m; L' is the length of the spring-finger, m; γ is the angle between the spring-finger and the crank, rad; φ is the swing angle of the cam mechanism, rad; φ_0 is the initial swing angle of the cam mechanism, rad; t is the time, s; R is the radius of the drum, m; ω picks up the speed of the disc, r/min.

Equation (8) for the radius of gyration of the end of the spring-finger R' is:

$$R' = X^2 + Y^2 \tag{8}$$

where R' is the radius of rotation of the end of the spring-finger, mm.

Without considering the oscillating motion of the spring-finger, the trajectory of the spring-finger is a cycloid, and the shape of the cycloid depends on the size of λ. The equation for the shape of the cycloid (9) is:

$$\lambda = \frac{R'\omega}{V_t} \tag{9}$$

The picking requirements can be met with a value of λ ranging from 0.17 to 0.58. Combined with the forward speed of the potato harvesting machinery in the agricultural machinery design manual and references, the forward speed of the picking device is controlled at 0.4 m/s ~ 0.8 m/s. Upon launch, a disc speed of 15~25 r/min was determined to be the best, a finding that laid the foundation for later tests [19,20].

2.4. Potato Trajectory Simulation Analysis

2.4.1. Simulation Model Building in EDEM

(1) Potato simulation modelling

In this study, the physical parameters of the 'purple-flowered white' potato were tested and analysed at harvest time. The results are shown in Table 1, with the average values for length-width-thickness being 92.59 mm, 63.71 mm and 41.46 mm respectively.

Table 1. Results of measurements of physical parameters of potatoes.

Potato Size	Length (mm)	Width (mm)	Thickness (mm)
Maximum value	149.0	100.7	85.3
Minimum value	71.4	59.2	43.8
Mean value	97.8	77.8	60.4

The spatial coordinates of the 5-sphere potato particles were set in the EDEM software as shown in Table 2, and the final 5-sphere potato particle model was created as shown in Figure 11. The potato particle model was then generated in the particle factory according to the law of normal distribution.

Table 2. Particle model parameters.

Name	Position X (m)	Position Y (m)	Position Z (m)	Physical Radius (m)
sphere 0	−0.02	0	0	0.03
sphere 1	0	−0.008	0	0.032
sphere 2	0	0.008	0	0.032
sphere 3	0.02	0	0	0.03
sphere 4	0	0	0	0.033

(2) Soil simulation modelling

In order to determine the parameters of the sandy soil in the potato growing area, a soil with 6% moisture content was used as the test soil sample and the soil parameters for

the simulation tests were determined by a combination of measurements and literature review [21,22] as shown in Table 3.

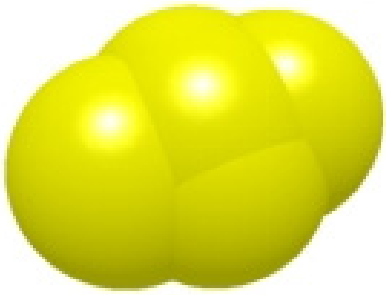

Figure 11. Potato particle model.

Table 3. Soil parameters.

Parameters	Numerical values
Poisson's ratio	0.2
Modulus of elasticity	13.5 MN/m^2
Density	1.38 g/cm^3
Coefficient of static friction	0.81
Coefficient of rolling friction	0.2095
Resting angle	35.53°
JKR surface energy coefficient	0.356

After practical research, the potato excavator passed through a soil with soft, non-bonded conditions. To facilitate modelling and reduce unnecessary calculations in the simulation, a single sphere soil particle model was established with a particle radius of 2 mm, as shown in Figure 12.

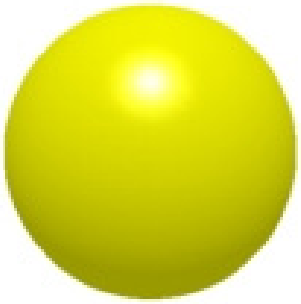

Figure 12. Single sphere particles.

(3) Soil trough simulation modelling

In this experiment, a soil trough with a length, width and height of 2000 × 500 × 300 mm was built with a model number of 50,000 soil particles and a model number of 50 potatoes. The Hertz-Mindlin with JKR model was selected for the discrete element contact model and a simplified pickup model was built as shown in Figure 13.

(4) Determination of contact parameters

In the simulation tests there was contact between soil and soil, soil and potato, potato and potato, pickup device and soil, and pickup device and potato. The material contact parameters can be collated from the literature [23] as shown in Table 4.

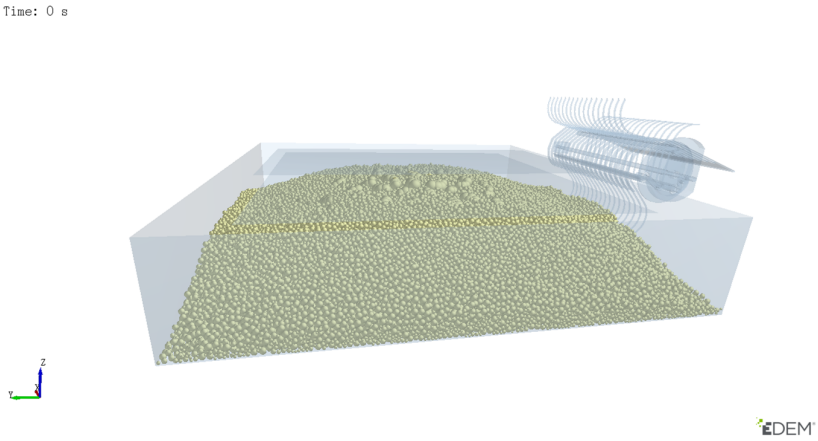

Figure 13. Soil channel model generated by EDEM pre-processing.

Table 4. Physical contact parameters.

Material	Recovery Coefficient	Static Friction Coefficient	Rolling Friction Coefficient
Potato-Potato	0.13	0.2	0.01
Potato-Soil	0.06	0.5	0.01
Potato-Pickup device	0.45	0.5	0.43
Soil-Soil	0.15	0.81	0.15
Soil-Pickup device	0.30	0.5	0.05

2.4.2. Building a Motion Simulation Model in Adams

The 3D model of the potato picking mechanism was simplified as shown in Figure 14. A simulation run was carried out using Adams software to make sure that the settings were correct, then the model building in Adams was ended and subsequent tests were carried out while keeping the machine stable.

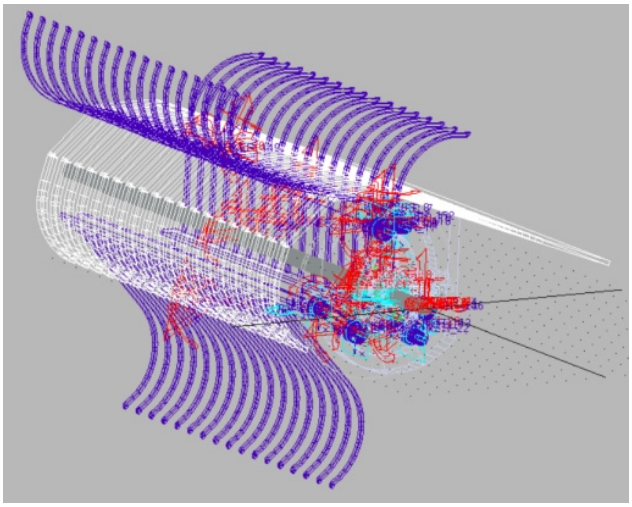

Figure 14. Model of the pickup device in Adams.

2.4.3. ADAMS-EDEM Coupled Analysis Test

A joint ADAMS and EDEM simulation model was established to analyse the potato trajectory and to verify the rationality of the spring-finger potato picker. A forward speed of 0.4 m/s and a spring-finger speed of 25 r/min were chosen. The EDEM software post-processing module can record the movement of the potatoes in real time while simulating

the picking process of the picking model. As shown in Figure 15, at 0.600021 s, the spring-finger comes into contact with the potatoes, at 1.30003 s, the potatoes are lifted to the uniformly rising stage, and at 2.00003 s, the potatoes enter the pushing and unloading stage. Then, at 2.40002 s, the potatoes are separated from the spring-finger and continue to move in the opposite direction until fall into the potato collection box, completing the potato picking process. The potatoes are picked up from the surface and lifted to the highest point reached during the process. The trajectory of the potatoes is related to the forward speed of the picker and the speed of the spring-finger.

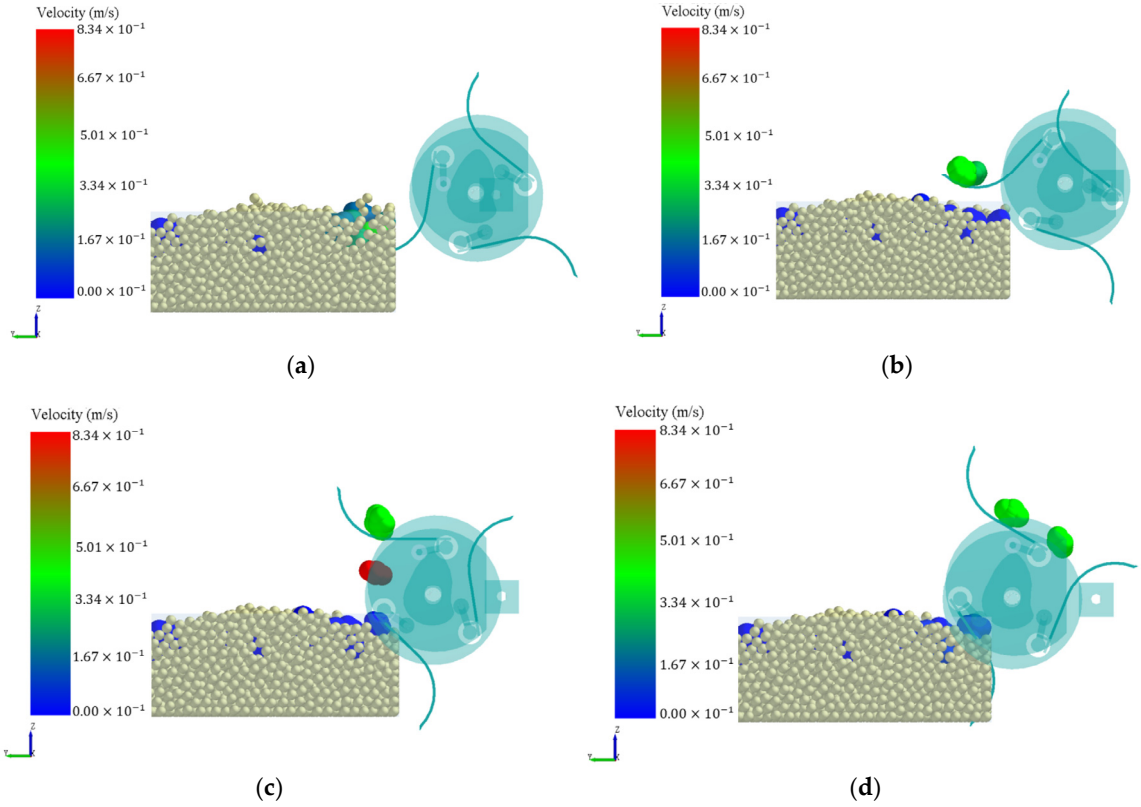

Figure 15. Potato trajectory diagram. (**a**) T = 0.600021 s. (**b**) T = 1.30003 s. (**c**) T = 2.00003 s. (**d**) T = 2.40002 s.

2.5. Laboratory Test

2.5.1. Test Conditions

Performance tests of the spring-finger picker were conducted in May 2022 in the soil tank laboratory of Inner Mongolia Agricultural University. According to the design requirements of the spring-finger picker, the soil should be prepared with a rotary tiller before the picking device works to ensure a consistent environment and ensure that the soil is loose and level. The test procedure is shown in Figure 16.

2.5.2. Evaluation Indicators

Referring to the index requirements in NY/T648-2015 "Technical specification for quality evaluation of potato harvesters" [24] issued by the Ministry of Agriculture of the People's Republic of China, the loss rate and woundedness rate were selected as the evaluation indexes of the spring-finger picking device.

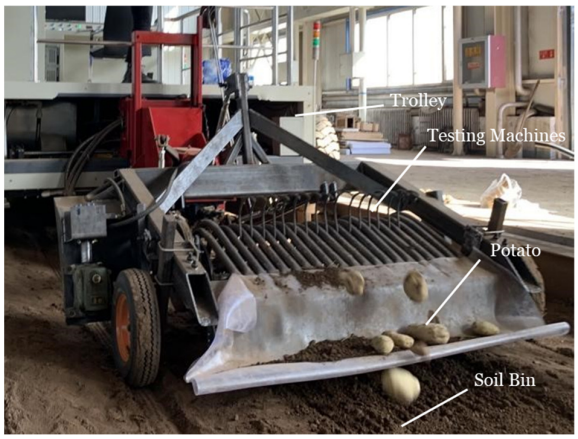

Figure 16. Laboratory test procedure.

(1) Original wounded potato rate: all test potatoes are weighed before the picking operation begins, from which the wounded potatoes are identified and weighed, and the weight of the wounded potatoes in the test area is calculated as a percentage of the total weight of potatoes in the test area, the value of which is the original wounded potato rate calculated according to Equation (10):

$$L_1 = \frac{Q_1}{Q} \times 100\% \tag{10}$$

where L_1 is the original wounded potato rate, %; Q_1 is the original wounded potato quality, kg; and Q is the total potato mass, kg.

(2) Loss rate: after operating the picking device, collect the potatoes that were picked up by the machine and the potatoes missed in the test area and weigh them separately. Calculate the percentage of missed potatoes in the test area to the total potato weight (potatoes picked up by the machine and missed potatoes), and take the value as the loss rate, calculated according to formula (11):

$$L_2 = \frac{Q_2}{Q_2 + Q_3} \times 100\% \tag{11}$$

where L_2 is the loss rate, %; Q_2 is the mass of missed potatoes, kg; and Q_3 is the mass of potatoes picked up by the machine, kg.

(3) Wounded rate: after the device has completed its picking operation, collect the potatoes in the test area (potatoes in potato boxes and missed potatoes) and weigh them. Then, find the wounded potatoes and weigh them. Calculate the percentage of wounded potatoes to the total potato weight, take the value and subtract the original wounded potato rate to obtain the wounded potato rate, calculated according to formula (12):

$$L_3 = \frac{Q_4}{Q_2 + Q_3} \times 100\% - L_1 \tag{12}$$

where L_4 is the percentage of wounded potatoes, %, and Q_4 is the mass of wounded potatoes, kg.

3. Results and Discussion

3.1. Experimental Scheme and Results

Combined with Design-Expert software, the response surface BBD method experimental design [25,26] was carried out, and the spring-finger speed, forward speed and embedded depth were selected as the main influencing factors. The speed of the spring-finger was set at 15–25 r/min, the forward speed at 0.4–0.8 m/s, and the embedded depth at 60–80 mm, and the table of test factor levels is shown in Table 5:

Table 5. Levels and codes of experimental variables.

Level	Test Factors		
	Spring-Finger Speed A (r/min)	Forward Speed B (m/s)	Embedded Depth C (mm)
−1	15	0.4	60
0	20	0.6	70
1	25	0.8	80

The BBD test was chosen for this trial in order to reduce the number of trials. 17 groups of trials were conducted, each group was repeated three times and the final mean was selected in order to take into account the interaction of all factors, with loss rate and wounded potato rate as indicators. The results of the trials are shown in Table 6 below:

Table 6. Design and results of the orthogonal test in the numerical simulation.

Test Number	Test Factors			Test Indicators	
	A r/min	B m/s	C mm	Y_1 %	Y_2 %
1	25	0.8	70	4.34	15.75
2	20	0.4	80	4.56	13.56
3	15	0.4	70	4.72	11.42
4	20	0.8	60	1.77	16.95
5	20	0.6	70	0.47	6.61
6	20	0.8	80	3.04	11.14
7	15	0.8	70	3.16	19.14
8	20	0.6	70	0.36	7.04
9	25	0.6	80	4.32	14.85
10	20	0.6	70	2.04	6.36
11	25	0.4	70	3.39	21.37
12	20	0.6	70	1.06	5.2
13	15	0.6	80	5.07	10.08
14	20	0.4	60	3.01	19.15
15	20	0.6	70	1.34	5.66
16	25	0.6	60	2.66	22.19
17	15	0.6	60	3.52	15.59

3.2. Analysis of Test Results

Using Design Expert12 software multiple regression fitting analysis of the data in Table 6, a quadratic polynomial response surface regression model was established for the three independent variables, loss rate, wounded potato rate, for the spring spring-finger speed A, forward speed B, and embedded depth C. The mathematical model (13) was:

$$\begin{cases} Y_1 = 1.05 - 0.22A - 0.42B + 0.75C + 0.63AB + 0.028AC - 0.070BC + 1.82A^2 + 1.03B^2 + 1.02C^2 \\ Y_2 = 99.77 - 2.02A + 0.74B + 2.28C + 2.71AB + 0.43AC + 0.31BC - 7.43A^2 - 6.16B^2 - 4.91C^2 \end{cases} \quad (13)$$

ANOVA was conducted on the model and the results are shown in Table 7. The p-values of the models for loss rate and wounded potato rate were less than 0.01 and the p-values of the misfit terms were greater than 0.05. The model coefficients of determination R2 were 0.9235 for loss rate and 0.9786 for wounded potato rate respectively, which shows that the optimised regression model was extremely significant and a good fit, and the model was reliable.

Table 7. Analysis variance table of test results.

Source of Variance	Loss Rate Y_1%					
	Sum of Squares	**Freedom**	**Mean Square**	**F-Value**	***p*-Value**	**Significance**
Model	33.09	9	3.68	9.39	0.0037	**
A	0.39	1	0.39	0.99	0.3531	
B	1.42	1	1.42	3.63	0.0986	*
C	4.55	1	4.55	11.61	0.0113	
AB	1.58	1	1.58	4.02	0.0849	*
AC	0.003025	1	0.003025	0.007728	0.9324	
BC	0.020	1	0.020	0.050	0.8293	
A^2	13.99	1	13.99	35.75	0.0006	**
B^2	4.43	1	4.43	11.31	0.0120	
C^2	4.34	1	4.34	11.09	0.0126	
residuals	2.74	7	0.39			
fail to fit	0.86	3	0.29	0.61	0.6415	
error	1.88	4	0.47			
total	35.83	16				
Source of Variance	**Wounded Potato Rate Y_2%**					
	Sum of Squares	**Freedom**	**Mean Square**	**F-Value**	***p*-Value**	**Significance**
Model	502.23	9	55.80	35.55	<0.0001	**
A	40.19	1	40.19	25.60	0.0015	**
B	0.79	1	0.79	0.51	0.5000	
C	73.51	1	73.51	46.83	0.0002	**
AB	44.49	1	44.49	28.34	0.0011	**
AC	0.84	1	0.84	0.53	0.4889	
BC	0.012	1	0.012	0.007709	0.9325	
A^2	132.60	1	132.60	84.48	<0.0001	**
B^2	110.99	1	110.99	70.71	<0.0001	**
C^2	63.77	1	63.77	40.63	0.0004	**
residuals	10.99	7	1.57			
fail to fit	8.80	3	2.93	5.36	0.0692	
error	2.19	4	0.55			
total	513.22	16				

Note: * indicates general significance, $0.05 < p < 0.1$; ** indicates highly significant, $p < 0.01$.

3.3. Response Surface Analysis

Response surface plots were obtained using Design Expert12 software as shown in Figures 17 and 18 to further investigate the effect law of the test factors (spring spring-finger speed A, forward speed B and embedded depth C) and their interaction on the test fingers (loss rate, wounded potato rate).

Figure 17 shows the loss rate Y1 interaction factor response surface analysis. Decreasing the spring-finger speed A and decreasing the forward speed B can reduce the loss rate; however, when the loss rate reaches an extreme point, the loss rate increases as the speed A of the picking gears and the forward speed B of the machine decrease. Decreasing the embedded depth C and increasing the spring-finger speed A can reduce the loss rate; after the loss rate reaches the extreme value, the loss rate will increase as the spring-finger speed A increases and the embedded depth C decreases. Moreover, increasing the forward speed B and decreasing the embedded depth C can help reduce the loss rate; however, when the loss rate reaches a very small value, the loss rate will increase as the forward speed B increases and the embedded depth C decreases.

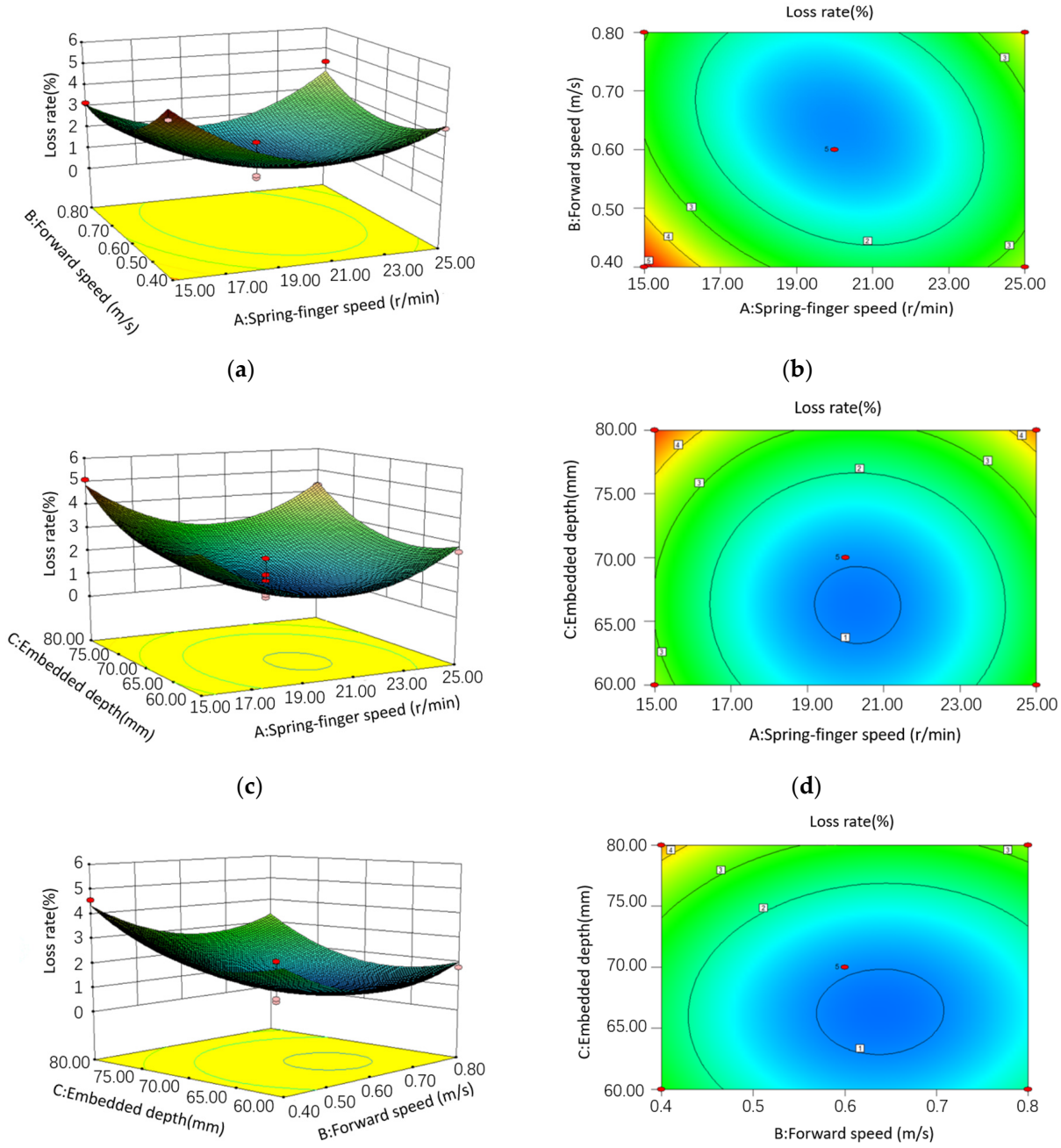

Figure 17. Loss rate interaction factor response surface analysis: (**a**) response surface plot of the effect of spring-finger speed and forward speed on the interaction of the loss rate (**b**) contour plot of the interaction between spring-finger speed and forward speed on the loss rate (**c**) response surface diagram of the interaction between spring-finger speed and embedded depth on the loss rate (**d**) contour plot of the interaction between spring-finger speed and embedded depth on the loss rate (**e**) response surface plot of the interaction between forward speed and embedded depth on the loss rate (**f**) contour plot of the interaction between forward speed and embedded depth on the loss rate.

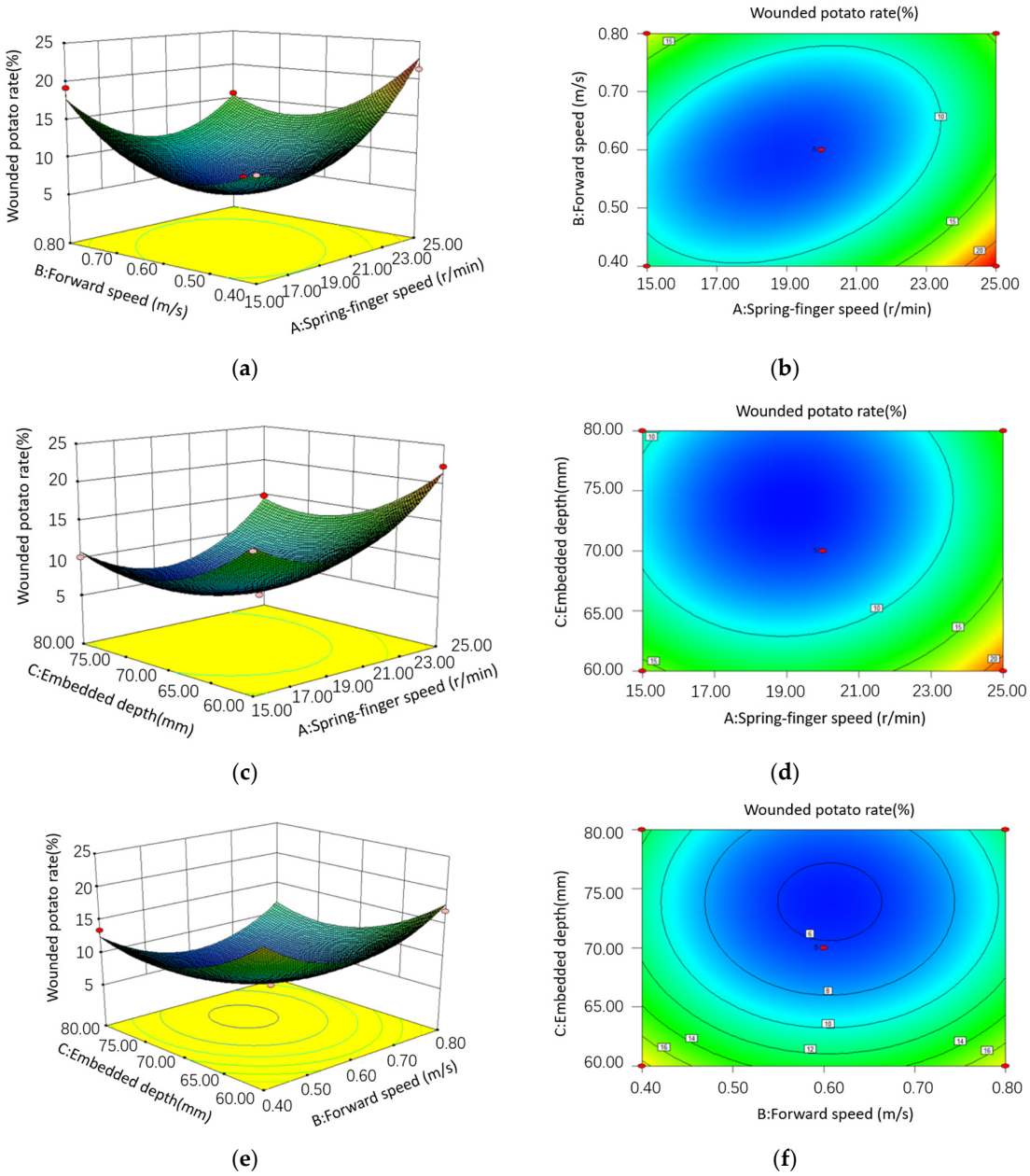

Figure 18. Response surface analysis of interactive factors on the wounded potato rate: (**a**) response surface plot of the effect of spring-finger speed and forward speed on the interaction of the wounded potato rate (**b**) contour plot of the interaction between spring-finger speed and forward speed on the wounded potato rate (**c**) response surface diagram of the interaction between spring-finger speed and embedded depth on the wounded potato rate (**d**) contour plot of the interaction between spring-finger speed and embedded depth on the wounded potato rate (**e**) response surface plot of the interaction between forward speed and embedded depth on the wounded potato rate (**f**) contour plot of the interaction between forward speed and embedded depth on the wounded potato rate.

Figure 18 shows the response surface analysis of the interaction factors for wounded potato rate. It can be seen that reducing the forward speed B and the spring-finger speed A helps to reduce the wounded potato rate. Decreasing the rotational speed of the spring spring-finger A and increasing the embedded depth C reduces the rate of wounded potatoes. Increasing the embedded depth C and decreasing the forward speed B helps to reduce the woundedness rate; however, when the wounded rate reaches a very small value, continuing

to decrease the forward speed B and continuing to increase the embedded depth C causes the woundedness rate to gradually increase.

3.4. Optimization Model Analysis and Laboratory Test Validation

Based on the aforementioned results of the regression model of the test indicators and the conditions of picking operation of the potato picking device, the constraints of each test factor were set in the Design Expert12 software, with the objective function shown in Equation (14). The optimum combination of parameters was found to be 19.57 r/min for the spring-finger speed, 0.61 m/s for the forward speed and 71.31 mm for the embedded depth, with corresponding loss rates of 1.18% and 5.71% for the wounded potato rate.

$$\begin{cases} \begin{matrix} minY_1 = f_1(A,B,C) \\ minY_2 = f_2(A,B,C) \end{matrix} \\ S.T. \begin{cases} \begin{matrix} Y_1 \le 5\% \\ Y_2 \le 6\% \end{matrix} \\ \begin{matrix} 5\ \text{r/min} \le A \le 45\ \text{r/min} \\ 0.2\ \text{m/s} \le B \le 1.6\ \text{m/s} \\ 50\ \text{mm} \le C \le 100\ \text{mm} \end{matrix} \end{cases} \end{cases} \tag{14}$$

To verify the reliability of the model prediction results, the optimised parameters were rounded and then subjected to a validation test, setting the spring-finger speed at 20 r/min, the forward speed at 0.6 m/s and the embedded depth at 70 mm. The test was carried out three times and the results were averaged, resulting in a loss rate of 1.48% and a wounded potato rate of 4.98%. The test verification results are in general agreement with the optimised analysis and can be used as the optimum working parameters for this picking mechanism.

4. Conclusions

(1) Aiming at the problems of low pickup rate and high wounded rate in potato sectional harvesting, a spring-finger potato picking device was designed, its working principle and key components were introduced, and the main design parameters of its components were determined by analysing key components such as spring-finger, drum disc, crank, roller and cam chute.

(2) The Box-Behnken response surface optimisation test method was used to analyse the effects of spring-finger speed, forward speed and embedded depth on the loss rate and wounded potato rate, to establish a regression model and to analyse their interaction, and the wounded potato rate was 4.98%. The results of the validation tests were basically consistent with the results of the optimisation analysis, indicating that the parameter optimisation regression model is reliable.

(3) Although the spring-finger potato picking device meets the design requirements of the picking process, there is still a certain wounded potato rate, and the subsequent research should improve the picking operation effect by optimising the profile of the cam slide.

Author Contributions: Conceptualization, L.W.; methodology, L.W. and F.L.; software J.Z. and J.L.; validation, L.W. and F.L.; investigation, X.Z. and J.L.; resources, L.W.; data curation, L.W. and Q.W.; writing—original draft, L.W. and X.F.; writing—review and editing, F.L. and S.X.; visualization, L.W. and F.L.; supervision, F.L.; funding acquisition, F.L. All authors have read and agreed to the published version of the manuscript.

Funding: This research was funded by the Science and Technology Program of Inner Mongolia Autonomous Region of China (2020GG0168), Inner Mongolia Autonomous Region Young Scientist Program of China (NJYT20B03), the National Natural Science Found of China (31901409) and the Science and Technology Research Project for Higher Education Institutions in Inner Mongolia Autonomous Region (NJZY21357).

Institutional Review Board Statement: Not applicable.

Data Availability Statement: Not applicable.

Conflicts of Interest: The authors declare no conflict of interest.

References

1. Mystkowska, I.; Zarzecka, K.; Gugała, M.; Ginter, A.; Sikorska, A.; Dmitrowicz, A. Impact of Care and Nutrition Methods on the Content and Uptake of Selected Mineral Elements in Solanum tuberosum. *Agronomy* **2023**, *13*, 690. [CrossRef]
2. Fan, J.; Li, Y.; Luo, W.; Yang, K.; Yu, Z.; Wang, S.; Hu, Z.; Wang, B.; Gu, F.; Wu, F. An Experimental Study of Stem Transported-Posture Adjustment Mechanism in Potato Harvesting. *Agronomy* **2023**, *13*, 234. [CrossRef]
3. Dou, Q.; Sun, Y.; Sun, Y.; Shen, J.; Li, Q. Domestic and foreign potato harvesting machinery status and development. *China Agric. Chem. News* **2019**, *9*, 206–210.
4. Zhao, Q. Domestic and foreign potato harvesting machinery research status and development prospects. *Agric. Eng.* **2020**, *6*, 7–10.
5. Luo, Q.; Lun, L.; Gao, M. Strategic pathways for high-quality development of China's potato industry from 2021 to 2025. *China Agric. Resour. Zoning* **2022**, *3*, 37–45.
6. Wei, Z.; Li, X.; Zhang, Y.; Li, H.; Sun, C. Research progress of potato full mechanized production technology and equipment. *Agric. Mech. Res.* **2017**, *9*, 1–6.
7. Shi, Y.; Yan, S.; Zhu, R.; Li, J.; Huang, S.; Liu, Y. Development and experiment of a small potato picker. *Arid Reg. Agric. Res.* **2016**, *4*, 287–291+298.
8. Xiao, W.; Gao, Y.; Chen, H.; Zhang, Y. Design and experiment of small potato picking and grading machine. *Agric. Mech. Res.* **2019**, *12*, 130–134.
9. Hu, Q.; Xiao, W. Design and test of an integrated potato picking and grading harvester. *Agric. Mech. Res.* **2021**, *11*, 110–114.
10. Liu, J.; Wei, M.; Kang, H.; Wang, Y.; Zhou, J. Design and experiment of potato harvester based on roller separation. *Agric. Mech. Res.* **2021**, *5*, 96–103.
11. Wang, W. Experimental Research on Potato Picking Device Based on Discrete Elements. Master's Thesis, Northwest University of Agriculture and Forestry Science and Technology, Shanxi, China, 2017.
12. Yang, J.; Li, G.; Hao, L.; Chen, W.; Ye, T. Research on the development status and main function structure of potato picker. *Agric. Mach. Use Maint.* **2019**, *3*, 15–16.
13. Wei, Z.; Wang, X.; Li, X.; Wang, F.; Li, Z.; Jin, C. Design and test of a self-propelled sorting potato harvester with crawler. *J. Agric. Mach.* **2023**, *2*, 95–106.
14. Campbell, A.J.; Birt, I.; MacKinnon, B. Modifications of a potato harvester for small plot field research. *Am. Potato J.* **1990**, *11*, 799–803.
15. Zhang, F.; Qiu, Z.; Mao, P. The model and simulation of the potato harvester. *Appl. Mech. Mater.* **2011**, *44*, 900–904. [CrossRef]
16. Yang, F.; Sun, B.; Zheng, S. Research status and development trend of potato harvesting machine. *For. Mach. Woodwork. Equip.* **2021**, *10*, 4–10.
17. Sheng, K.; Zeng, N. Mechanism characteristics and mathematical model of motion of a spring-tooth roller picker. *J. Agric. Mach.* **1991**, *1*, 51–57.
18. Yang, H.; Hu, Z.; Wang, B. Research progress of potato harvesting mechanization technology. *Chin. J. Agric. Mach. Chem.* **2019**, *11*, 27–34.
19. China Agricultural Machinery Research Institute. *Handbook of Agricultural Machinery Design*; Machinery Industry Press: Beijing, China, 2007; p. 1056.
20. Kanafojski, T. *Crop-Harvesting Machines*; China Agricultural Machinery Press: Beijing, China, 1983; pp. 487–512.
21. Sun, Y.; Shao, L.; Fan, Z. Experimental study on Poisson's ratio of non-cohesive soils. *Geotechnics* **2009**, *s1*, 63–68.
22. Song, Z.; Li, H.; Yan, Y. Calibration and testing of a discrete element simulation model for non-equal-sized particles in mulberry soils. *J. Agric. Mach.* **2022**, *6*, 21–33.
23. Wang, Y. Research on the Structure and Loosening Effect of Deep Loosening Shovel Based on Discrete Element Method. Master's Thesis, Jilin Agricultural University, Jilin, China, 2014.
24. *NY/T 648-2015*; Technical Specification for Quality Evaluation of Potato Harvesters. China Standard Press: Beijing, China, 2015.
25. Chen, K. *Experimental Design and Analysis*; Tsinghua University Press: Beijing, China, 2005; pp. 123–134.
26. Pan, L.; Chen, J. *Experimental Design and Data Processing*; Southeast University Press: Nanjing, China, 2008; pp. 78–86.